

Noise Detection for Biosignals Using an Orthogonal Wavelet Packet Tree Denoising Algorithm

Manuel Schimmack and Paolo Mercorelli

Abstract—This article deals with the noise detection of discrete biosignals using an orthogonal wavelet packet. In specific, it compares the usefulness of Daubechies wavelets with different vanishing moments for the denoising and compression of the digitalised biosignals in case of surface electromyography (sEMG) signals. The work is based upon the discrete wavelet transform (DWT) version of wavelet package transform (WPT). A noise reducing algorithm is proposed to detect unavoidable noise in the acquired data in a model independent way. The noise of a signal sequence will be defined by a seminorm. This method was developed for a possible observation during a fracture healing period. The proposed method is general for signal processing and its design was based upon the wavelet packet.

Keywords—noise detection, wavelet packet transform, wavelet analysis, Daubechies wavelet, linux-based embedded system, ARM processor platform

I. INTRODUCTION

WAVELETS are used in a wide range of applications for biomedical signal and image processing and in the fields of electrocardiography, electroencephalography, and electromyography, as well as for the algorithms for magnetic resonance imaging or positron emission tomography applied in biomedical image processing [1]. The control of active prostheses for human limbs with algorithms for classification and reliable signal pattern recognition is another important field of application [2]. This article presents a wearable embedded system to observe the activity of an injured forearm during rehabilitation, including the feedback which is not detectable by an accelerometer. The aim is to record the movements of the extremity, which is stabilized in a reusable orthosis. Therefore, a wearable measurement system was constructed to detect the biosignals [3] and [4]. In general, the sEMG signal provides information about the performance of muscles and nerves [5], [6], also in the context of neurological diagnosis of myopathies and neuropathies.

Signal and data conditioning followed using wavelets for active denoising and data compression. This focuses upon on a portable Linux-based embedded system together with the use of Haars and Daubechies wavelets within the context of the digitalization of sEMG signals [7]. More specifically, it compares the usefulness of Daubechies wavelets with different vanishing moments for the denoising and

compression of the digitalised biosignals. In [8], the calculation of the signal projection coefficients based on the signal interpolation is proposed by means of cubic B-splines.

A noise reducing algorithm is proposed to detect unavoidable noise in the acquired data. With the help of a seminorm the noise of a sequence is defined. Using this norm it is possible to rearrange the wavelet basis, which can illuminate the differences between the coherent and incoherent parts of the sequence, where incoherent refers to the part of the signal that has either no information or contradictory information.

The structure of the contribution is the following. Section II devided some background aspects of the orthogonal wavelets in context of the vanishing moment and the computation. Section III presents a wavelet based denoising algorithm and describes it in a graphical and in an analytical way. Before the conclusion, the measurement procedure is shown in Section IV. The implementation in a Linux-based embedded system and its validation in a case study through simulations is presented in V.

MAIN NOMENCLATURE

b :	frequency-dependent parameter
c_n :	wavelet coefficients
Db :	Daubechies wavelet index
D :	wavelet tree depth
d :	index scale
$e(t)$:	noise
l :	interval of time
k :	time-dependent parameter
$\mathcal{L}(\omega)$:	trigonometric polynomial
$m_0(\omega)$:	generating function
N :	vanishing moment
n :	samples
$y(t)$:	biosignal
$P_N(\omega)$:	polynomial
$S_{(d,b,k)}$:	wavelet coefficient
V :	vector space
$wP_{(d,b,k)}$:	wavelet coefficient tree
λ :	scalar
$\psi^n(t)$:	wavelet family
z :	discrete complex variable
ω :	angular frequency

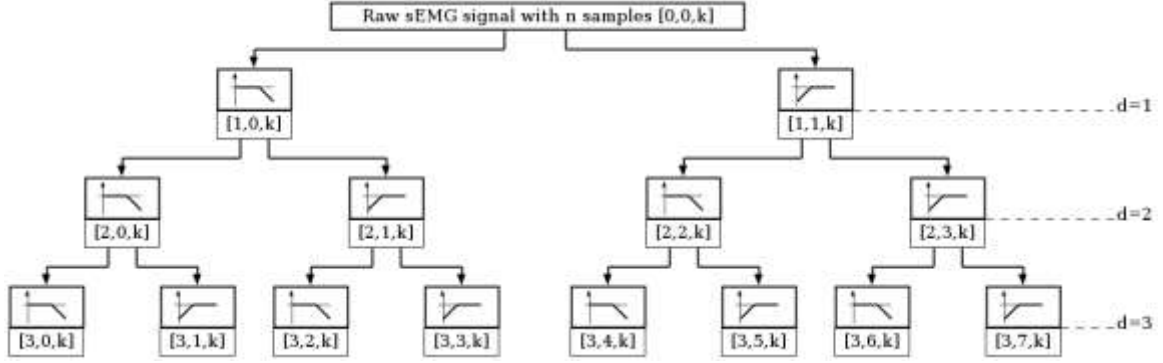


Fig. 1. Input-signal and the wavelet coefficients in a tree-like structure with the scale index d , the time translation parameter parameter k and different values of the phase parameter b

II. ORTHOGONAL WAVELET PACKET TREE

A. Haars wavelet

One of the first orthogonal wavelets was the Haars wavelet. In this case very short discrete signals can be used, following the example of [9]. To give a concise overview on the Haar wavelet a function

$$\psi_{(d,b,k)}(t) = \psi_b(2^d t - n) \quad (1)$$

is considered with a support of size 2^{-d} of the Nyquist frequency. For the two properties of the Haar basis follows:

- the $\psi_{(d,b,k)}^h(t)$ are orthonormal;
- any $\mathcal{L}^2(\mathbb{R})$ function $f(t)$ can be approximated, up to arbitrarily low precision, by a finite linear combination of the $\psi_{(d,b,k)}^h(t)$.

The weighted coefficients $wp_{(d,b,k)}$ are calculated as follows

$$wp_{(d,b,k)} = \int_I f(t) \psi_{(d,b,k)}^h(t) dt. \quad (2)$$

For $b = 0$ it is possible to define the following coefficients

$$s_{(d,0,k)} = \int_I f(t) \psi_{(d,0,k)}^h(t) dt, \quad (3)$$

where I is the considered interval of time, $f(t)$ is the required signal, and $\psi_{(d,0,k)}^h(t)$ is the mother function of Haars wavelet [10]. To conclude

$$f(t) = \sum_k s_{(d,0,k)} \psi_{(d,0,k)}^h(t) + \sum_b \sum_k wp_{(d,b,k)} \psi_{(d,b,k)}^h(t), \quad (4)$$

where $s_{(d,k)} = wp_{(d,0,k)}$. The Haar functions are identified using the parameter tuple, (d, b, k) , here $d = 1$ represents the highest degree of refinement with respect to time. The wavelet packets "MakeWaveletPacket", which comes from the

Wavelab Version 850 of Stanford University [11], is represented by the indexes (d, b, k) . Figure 1 shows the corresponding tree with the wavelet coefficients, described by $wp_{(d,b,k)}$. It represents the contribution of each of the wavelets to the signal based on n samples. The notation $wp_{(1,0,0, \dots, \frac{n}{2}-1)}$ denotes the coefficients on the first level on the left with time shifts 0 through $\frac{n}{2} - 1$.

B. Daubechies wavelet

An established methods for sEMG signal analysis is the Daubechies (Db) wavelet, which is used in [12], [13], [14]. The computation of the Daubechies wavelet require a polynomial with binomial coefficients as follows

$$P_N(t) = \sum_{k=0}^{N-1} \binom{N-1+k}{k} x^k, \quad (5)$$

where ψ^{Db} has N vanishing moments. For the response of time and frequency for the Daubechies wavelet, it also needs a trigonometric polynomial, as shown below

$$\mathcal{L}(\omega) = \sum_{k=0}^n b_k \cdot e^{-jk\omega}. \quad (6)$$

The generating function, also known as transfer function is defined as follows

$$m_0(\omega) = \left(\frac{1 + e^{-j\omega}}{2} \right)^N \mathcal{L}(\omega), \quad (7)$$

being $m(\omega)$ defined as

$$m(\omega) = \frac{1}{\sqrt{2}} \sum_{n=-\infty}^{\infty} c_n \cdot e^{-jn\omega}. \quad (8)$$

Ingrid Daubechies was the first to construct compactly orthogonal wavelets with a modifiable degree of smoothness. This smoothness is based on the quantity of coefficients and is connected to the level of the vanishing moment N . According to the references of Daubechies in Chapters 6 and 7 in [15], a vanishing moment can be described by the following relation

$$\int x^n \psi(t) dt = 0, \quad n = 0, 1, \dots, N-1. \quad (9)$$

Using the relationship between (7) and (8), it is possible to calculate the wavelet coefficients c_n . According to (5) and (6), for a vanishing moment of $N = 1$, the polynomial can be expressed as follows

$$P_1(t) = \sum_{k=0}^0 \binom{k}{k} x^k = 1, \quad (10)$$

and the trigonometric polynomial is defined as

$$\mathcal{L}(\omega) = \sum_{k=0}^0 b_k \cdot e^{-jk\omega} = 1. \quad (11)$$

For the generating function with (7) it follows that

$$m_0(\omega) = \frac{1}{2}(1 + e^{-j\omega}). \quad (12)$$

Based on (12), the Daubechies wavelet behaves like a Haars wavelet in the frequency domain with a vanishing moment of $N = 1$. According to (5) and (6), for a vanishing moment of $N = 2$ the following polynomial is obtained

$$P_2(t) = \sum_{k=0}^1 \binom{1+k}{k} x^k = 1 + 2x, \quad (13)$$

combined with

$$\mathcal{L}(\omega)\mathcal{L}(-\omega) = \sum_{k=0}^n b_k \cdot e^{-jk\omega} = 2 - \frac{1}{2}(e^{j\omega} + e^{-j\omega}). \quad (14)$$

Substitute (8) in (6) and if (14) $z = e^{-j\omega}$ it follows that

$$P_2(z) = \frac{1}{2} \sum_{k=-1}^1 a_{|k|} z^{1+k} \frac{1}{2} (-1 + 4z - z^2) \frac{1}{2} (z - (2 + \sqrt{3})) (z - (2 - \sqrt{3})). \quad (15)$$

The square root of (15) is

$$\sqrt{\frac{1}{2} (1-1) \frac{1}{2 + \sqrt{3}}} = \frac{1}{\sqrt{2}} \sqrt{2 - \sqrt{3}} (z - (2 + \sqrt{3})) \frac{1}{2} (\sqrt{3} - 1) (z - (1 + \sqrt{3})). \quad (16)$$

The expression (16) must have the value of 1 at $z = 1$ or equivalently at $\omega = 0$. It follows for the generation function in (8) that

$$m_0(\omega) = \left(\frac{1 + e^{-j\omega}}{2} \right)^2 \frac{1}{2} \left((1 - \sqrt{3})e^{-j\omega} + (1 + \sqrt{3}) \right) \frac{1}{\sqrt{2}} \left(\frac{1 + \sqrt{3}}{4\sqrt{2}} + \frac{3 + \sqrt{3}}{4\sqrt{2}} e^{-j\omega} \frac{3 - \sqrt{3}}{4\sqrt{2}} e^{-2j\omega} + \frac{1 - \sqrt{3}}{4\sqrt{2}} e^{-3j\omega} \right). \quad (17)$$

Considering (17) for the implementation, the Daubechies wavelet coefficients with $N = 2$ becomes as follows

$$\begin{aligned} c_0 &= \frac{1}{4\sqrt{2}}(1 + \sqrt{3}), & c_1 &= \frac{1}{4\sqrt{2}}(3 + \sqrt{3}), \\ c_2 &= \frac{1}{4\sqrt{2}}(3 - \sqrt{3}), & c_3 &= \frac{1}{4\sqrt{2}}(1 - \sqrt{3}). \end{aligned} \quad (18)$$

III. AXIOMATIC SEMINORM WAVELET FOR A DENOISING METHOD

A. Seminorm

Definition 1: A observed sequence is defined as

$$y(t) = x(t) + e(t). \quad (19)$$

The incoherent part of the sequence $y(t)$ at every level d of the packet tree is defined as

$$e(t) = \sum_{(\mathbf{d}^*, \mathbf{b}^*)} \sum_{k=0}^{2^{D-d}} wp_{(\mathbf{d}^*, \mathbf{b}^*, k)} \psi_{(\mathbf{d}^*, \mathbf{b}^*, k)}(t), \quad (20)$$

where if a specified length n (dynadic length) is considered to determine the height of the wavelet tree $D = \log_2(n)$ and the selected wavelets are characterised by the indexes $(\mathbf{d}^*, \mathbf{b}^*)$ such that

$$\{(\mathbf{d}^*, \mathbf{b}^*)\} = \arg \left(\min_{(d,b)} \left| \sum_{k=0}^{2^{D-d}} \{wp_{(d,b,k)}\} \right| : \{0 \leq k \leq 2^{D-d}, 0 < b \leq 2^d - 1, \forall d \in \mathbb{N}\} \right). \quad (21)$$

Being based on the expected signal noise considered in Def. 1, a seminorm is licit to be contemplated in order to discern the subspace which characterises noise $e(t)$. Here the definition of a seminorm is reported as it is well known from the literature.

Definition 2: Let $\mathbf{V} \in \mathbb{R}^n$ be a vector space and if function $p = \|\nu\|: \mathbb{R}^n \rightarrow \mathbb{R}^+$ satisfies all the following conditions for all $\nu \in \mathbf{V}$ and any scalar λ , then function $\|\nu\|$ represents a seminorm for the vector \mathbf{V} :

$$\|\nu\| > 0, \text{ for all } \nu \in \mathbf{V} \text{ (positivity),} \quad (22)$$

$$\|\lambda \cdot \nu\| = |\lambda| \cdot \|\nu\|, \text{ with } \lambda \in \mathbb{F} \text{ and } \nu \in \mathbf{V} \text{ (absolute homogeneity)} \quad (23)$$

and

$$\|\nu_1 + \nu_2\| \leq \|\nu_1\| + \|\nu_2\|, \text{ with } \lambda \nu \in \mathbf{V} \text{ (subadditivity).} \quad (24)$$

According to Def. 2 function

$$p(wp_{(d,b,k)}) = \left| \sum_{k=0}^{2^{D-d}} \{wp_{(d,b,k)}\} \right|, \quad (25)$$

is a seminorm where $wp_{(d,b,k)}$ are the wavelet coefficients for each of the packets (d,p,k) defined above. Function $p(wp_{(d,b,k)})$ satisfies the positivity, absolute homogeneity and subadditivity properties, not satisfying however the separation property required as a norm. $p(wp_{(d,b,k)}) = 0$ does not have to imply necessarily that the sequence (vector) $wp_{(d,b,k)} = 0$. According to Def. 1 the noise is defined as that part of the signal which consists either small or opposite terms. So using this norm, that incoherent part of the signal which comes from the oscillating components can be recognised by just looking at the minimum of this seminorm. In other words, the separation subspace in the field characterised by the tree of coefficients $wp_{(d,b,k)} \forall d,p,k$ is exactly the subspace of the noise.

B. Description of the algorithm and Signal cleaning procedure

Figure shows 2 the flow chart of the algorithm, which works in the following way. The main idea is to compare the defined axiomatic seminorm of the signal decomposition between fathers and sons through the tree. Starting in the second level of the tree $d = 2$ the algorithm looks for the minima. Once it is founded, the algorithm considers the sum of the seminorm of the sons in level $d = 3$. If the sum is less than the seminorm calculated at the father level $d = 2$, then the noise is located in the sons. If not, the noise is localised in the subspace of the father. Given the sampled biosignal

- **Step 1:** Specify dyadic length, n , in order to determine the height of the wavelet tree: $D = \log_2(n)$.
- **Step 2:** Construct the wavelet coefficient tree $wp_{(d,b,k)}$ for every $d, b > 0$ and for every k .
- **Step 3a:** For all time-frequency intervals such that $b = 1, 2, \dots, 2^d - 1$ with $d > 1$, calculate the absolute value of the \sum_k for all time-frequency intervals of the

tree, that is, $W \text{ sum}(d, b) = |\sum_k W(d, b)|$.

- **Step 3b:** For every "wavelet father" $W(d, b)$ at the node (d, b) with $b > 0$, calculate its left child at the node $(d + 1, bLeft)$ and its right child $(d + 1, bRight)$. Then, calculate the absolute value of the sum with respect to k and denote them as

$$W \text{ sumChildLeft} = \left| \sum_k W \text{ sum}(d, bLeft) \right| \quad (26)$$

and

$$W \text{ sumChildRight} = \left| \sum_k W \text{ sum}(d, bRight) \right|. \quad (27)$$

While ($d > D$)

For $b = 1: 2^d - 1$

If

$$W \text{ sum}(d, b) \leq W \text{ sumChildLeft} + W \text{ sumChildRight}$$

$$W_b(d^*, b^*) = \arg \left(\min_{(d,b)} W \text{ sum}(d, b) \right)$$

else

$$W_b(d^*, b^*) = \arg \left(\min_{(d,b)} W \text{ sumChildLeft} \right)$$

$$W_b(d^*, b^*) = \arg \left(\min_{(d,b)} W \text{ sumChildRight} \right)$$

End If

End b loop

End While – d loop

- **Step 4:** Reconstruct the noise:

$$e(t) = \sum_{(\mathbf{d}^*, \mathbf{b}^*) \in W_b} \sum_{k=0}^{2^{D-d}} wp_{p(\mathbf{d}^*, \mathbf{b}^*, k)} \psi_{p(\mathbf{d}^*, \mathbf{b}^*, k)}(t). \quad (28)$$

and reconstruct the denoised signal

$$y_d(t) = y(t) - \sum_{(d^*, b^*) \in W_b} \sum_{k=0}^{2^{D-d}} w_p(d^*, b^*, k) \psi_p(d^*, b^*, k)(t). \quad (29)$$

IV. METHODOLOGY AND EMBEDDED SYSTEM

A. Biosignal processing

Figure 3 shows the general block diagram of the portable Linux based embedded system with the standard interfaces and corresponding components, which works like a signal processing module. The system based on the Broadcom BCM2836 system on a chip (SoC) and has a quad-core ARM Cortex-A7 central processing unit (CPU) with a VideoCore IV dual-core graphics processing unit (GPU). The used Linux kernel for the operating system based on the ARM hard-float (armhf) Debian architecture. Using Ag/AgCl pH electrodes the amplifier stage of the four channel sEMG measurement system is comprised of low noise differential preamplifiers for the sEMG signals with integrated analog signal processing module (ASP).

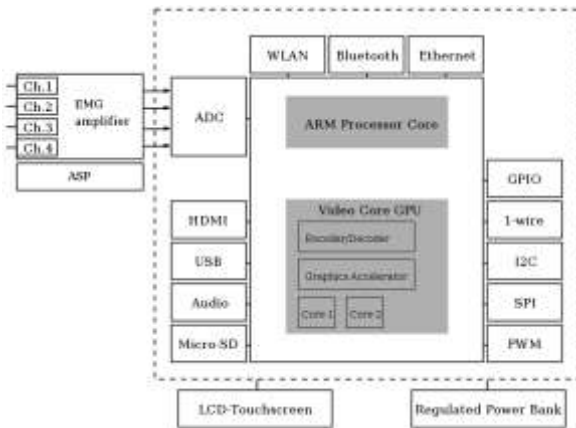


Fig. 4. General block diagram of the analog- and digital sEMG signal processing of the linux based embedded system

B. Data acquisition

Figure 5 shows the removable and flexible forearm orthoses with the Linux embedded measurement system. This medical device consists of an inner terry cloth sleeve for comfort and hygiene and a vacuum cushion containing soft beads supported by an orthosis that can be adjusted to hold the hand at different positions or to allow motion. The muscle activity during defined motions of the extremity while holding a 2 kg dumbbell was recorded. These motions flexed musculus biceps brachii, flexor digitorum profundus, extensor digitorum communis and flexor digitorum superficialis.



Fig. 5: Depiction of measurement system and portable Linux based embedded system

V. VALIDATION AND CASE STUDY

To compare the results obtained by Haar and Daubechies wavelets with different vanishing moments, the same seminorm used for the localisation of the noise is adapted to define the error

$$Error = \left| \sum_{k=1}^n x(k) - y_d(k) \right|. \quad (30)$$

Figure 6 shows the graphical representation of the test square wave signal with known Gaussian noise. The reconstruction based on different vanishing moments of the square wave signal, which are presented in Fig. 7. The recorded motion and activity of musculus biceps brachii is shown in Fig. 8 and also its reconstruction based on Haars wavelet is presented. Figure 9 shows the same biosignal with the Daubechies wavelet and vanishing moment $N = 2$. More in detail present Fig. 10 the results of the reconstruction based on m. biceps brachii using different vanishing moments. Figure 11 and Fig. 12 show the graphical representation in form of stairs plots and compare the sEMG reconstruction of M. extensor digitorum communis. After the analysis of the differer vanishing moments it results, that the different errors are quite close and offer the similar quality of approximation.

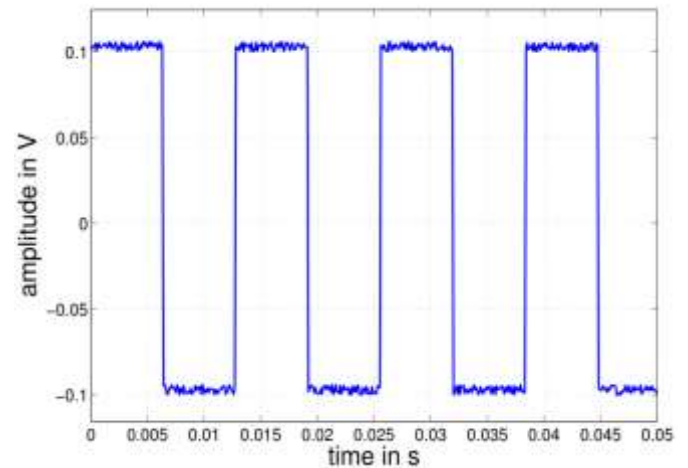


Fig. 6. Depiction of test square wave signal with Gaussian noise

VI. CONCLUSION

This contribution deals with the noise detection of discrete EMG signals using an orthogonal wavelet packet. More specifically, it compares the usefulness of Daubechies wavelets with different vanishing moments based on the discrete signals. new denoising procedure is proposed and validated by computer simulations by using GNU Octave and MATLAB/ /SIMULINK. The wavelet architecture based on the Wavelab Version 850 library of the Stanford University (USA). Due to the general structure of the proposed procedure, further work shute applications in difference scientific fields in the context of noise detection or vibrations recognition are going to be studied.

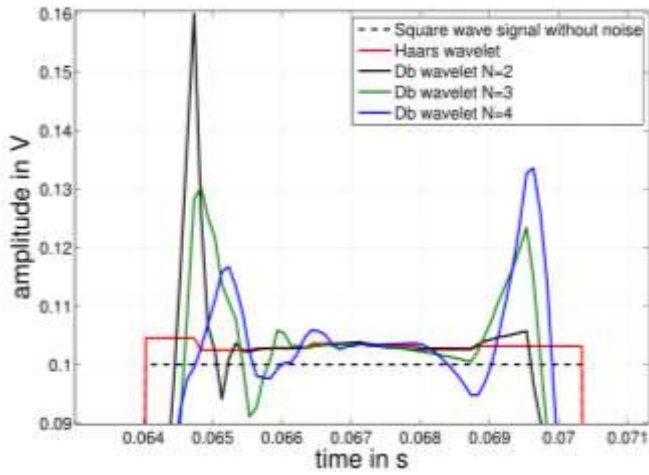


Fig. 7. Graphical representation of reconstruction of the square wave signal with different vanishing moments of Daubechies wavelet

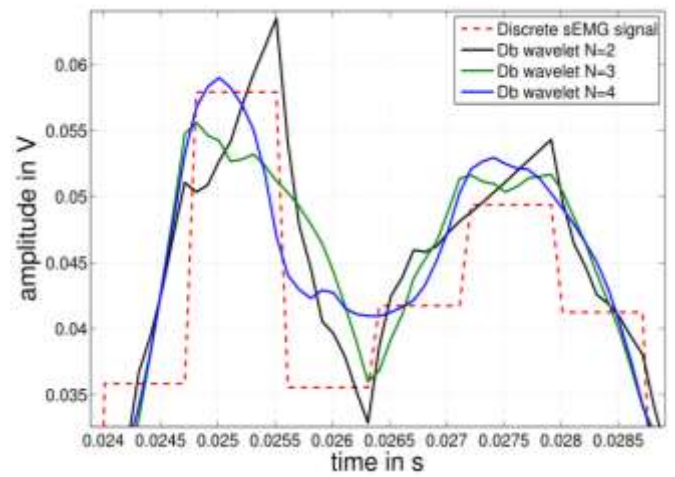


Fig. 10. Reconstruction of the m. biceps brachii signal using Daubechies wavelet with different vanishing moments

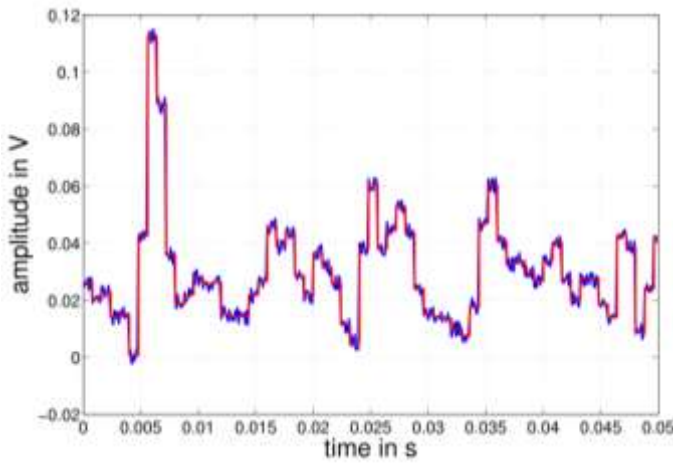


Fig. 8. Reconstruction of the m. biceps brachii signal using Haars wavelet

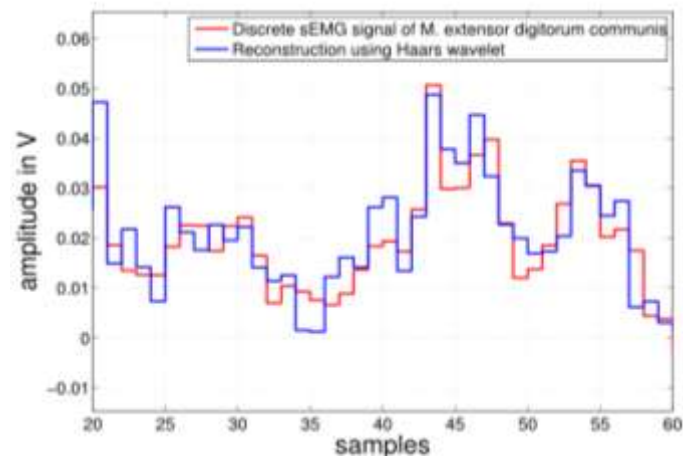


Fig. 11. Stairs plot of discrete sEMG signal using Haars wavelet

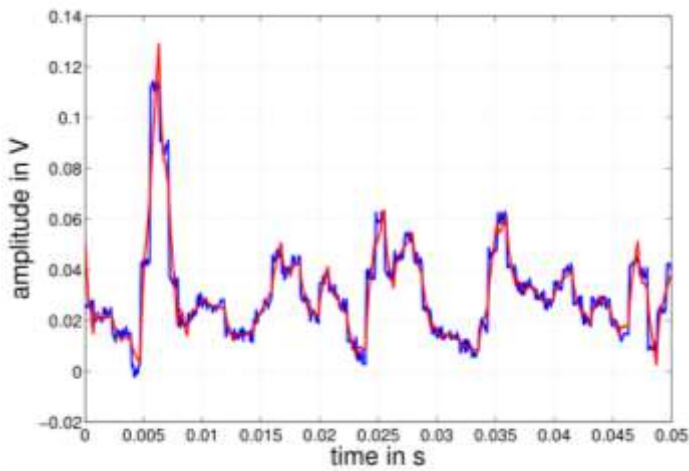


Fig. 9. Reconstruction of the m. biceps brachii signal using Daubechies wavelet with vanishing moment $N = 2$

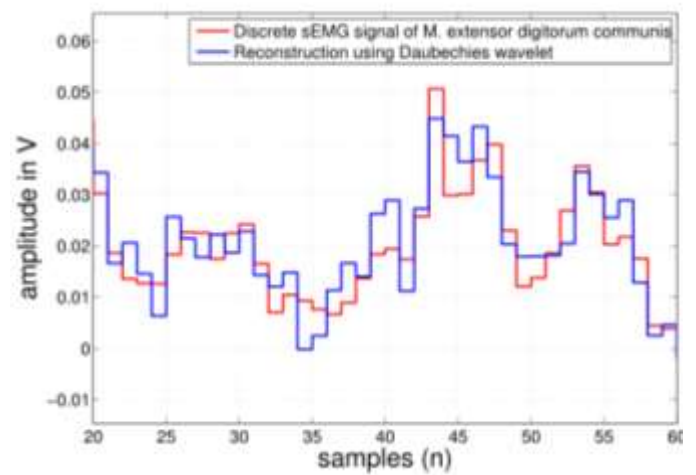


Fig. 12. Stairs plot of discrete sEMG signal using Daubechies wavelet

REFERENCES

- [1] S. Neville and N. Dimopoulos. Wavelet denoising of coarsely quantized signals. *IEEE Transactions on Instrumentation and Measurement*, 55(3):892–901, 2006.
- [2] J. Tomaszewski, T. G. Amaral, O.P. Dias, A. Wolczowski, and M. Kurzynski. EMG signal classification using neural network with AR model coefficients methods and models in automation and robotics. 14th International Conference on Methods and Models in Automation and Robotics, 14(1):318–325, 2009.
- [3] M. Schimmack and P. Mercorelli. Linux-based embedded system for wavelet denoising and monitoring of semg signals using an axiomatic seminorm. In *IFAC International Conference on Programmable Devices and Embedded Systems*, pages 278–283, Cracow, 2015.
- [4] M. Schimmack, A. Hand, P. Mercorelli, and A. Georgiadis. Using a seminorm for wavelet denoising of sEMG signals for monitoring during rehabilitation with embedded orthosis system. In *IEEE MeMeA - International Symposium on Medical Measurements and Applications*, Italy, 2015.
- [5] S. Shahid, J. Walker, G. M. Lyons, C. A. Byrne, and A. V. Nene. Application of higher order statistics techniques to EMG signals to characterize the motor unit action potential. *IEEE Transactions on Biomedical Engineering*, 52(7):1195–1209, 2005.
- [6] C.J.D. Luca. Physiology and mathematics of myoelectrical signals. *IEEE Transactions on Biomedical Engineering*, 26(6):313–325, 1979.
- [7] M. Unser and A. Aldroubi. A review of wavelets in biomedical applications. *Proceedings of the IEEE*, 84(4):626–638, 1996.
- [8] W. Rakowski. Prefiltering in wavelet analysis applying cubic B-splines. 14th International Conference on Methods and Models in Automation and Robotics, 60(4):331–340, 2014.
- [9] A. Frick and P. Mercorelli. System and methodology for noise level estimation by using wavelet basis functions in wavelet packet trees. European Patent Office under publication number: DE10225344, 2002.
- [10] P. Mercorelli and A. Frick. Noise Level Estimation Using Haar Wavelet Packet Trees for Sensor Robust Outlier Detection. Series: Lecture Note in Computer Sciences, Springer-Verlag publishers, 2006.
- [11] J. Buckheit, S. Chen, D. Donoho, I. Johnstone, and J. Scargle. About wavelab. *Handbook of WaveLab Version .850* by Stanford University and NASA-Ames Research Center, pages 1–37, 2005.
- [12] A. Phinyomark, A. Nuidod, P. Phukpattaranont, and C. Limsakul. Feature extraction and reduction of wavelet transform coefficients for emg pattern classification. *Electronics and Electrical Engineering*, 122(6):27–32, 2012.
- [13] C.-F. Jiang, Y.-C. Lin, and N.-Y. Yu. Multi-scale surface lectromyography modeling to identify changes in neuromuscular activation with myofascial pain. *IEEE Transactions on Neural Systems and Rehabilitation Engineering*, 21(1):89–95, 2013.
- [14] D. K. Kumar, N.D. Pah, and A. Bradley. Wavelet analysis of surface electromyography to determine muscle fatigue. *IEEE Transactions on Neural Systems and Rehabilitation Engineering*, 11(4):400–406, 2003.
- [15] I. Daubechies. *Ten Lectures On Wavelets*. SIAM: Society For Industrial And Applied Mathematics, 1992.